This paper is available on line at http://www.mcponline.org

Structurally Informative Tandem Mass Spectrometry of Highly Sulfated Natural and Chemoenzymatically Synthesized Heparin and Heparan Sulfate Glycosaminoglycans*[S]

Muchena J. Kailemia‡, Lingyun Li§, Yongmei Xu¶, Jian Liu¶, Robert J. Linhardt§, and I. Jonathan Amster‡‖

The highly sulfated glycosaminoglycan oligosaccharides derived from heparin and heparan sulfate have been a highly intractable class of molecules to analyze by tandem mass spectrometry. Under the many methods of ion activation, this class of molecules generally exhibits SO_3 loss as the most significant fragmentation pathway, interfering with the assignment of the location of sulfo groups in glycosaminoglycan chains. We report here a method that stabilizes sulfo groups and facilitates the complete structural analysis of densely sulfated (two or more sulfo groups per disaccharide repeat unit) heparin and heparan sulfate oligomers. This is achieved by complete removal of all ionizable protons, either by charging during electrospray ionization or by Na^+/H^+ exchange. The addition of millimolar levels of NaOH to the sample solution facilitates the production of precursor ions that meet this criterion. This approach is found to work for a variety of heparin sulfate oligosaccharides derived from natural sources or produced by chemoenzymatic synthesis, with up to 12 saccharide subunits and up to 11 sulfo groups. ***Molecular & Cellular Proteomics 12: 10.1074/mcp.M112.026880, 979–990, 2013.***

Heparin (Hp)[1] and heparan sulfate (HS) are linear, polydisperse, and highly sulfated glycosaminoglycans (GAGs), with a repeating disaccharide building block composed of a 1–4-linked glucosamine and a uronic acid residue (1). The saccharide residues may have a variety of modifications, and these are usually heterogeneous due to the nontemplate nature of their biosynthesis (2). Glucosamine residues may be substituted with *N*-sulfo or *N*-acetyl and 3- and/or 6-*O*-sulfo groups. Uronic acid residues can be either glucuronic or iduronic acid and substituted with 2-*O*-sulfo groups (3, 4). These structural features are thought to control Hp and HS biological activity, *e.g.* their interactions with proteins, and so the structural characterization of GAGs is an important target for chemical analysis (1, 5, 6). A particularly well known example of a GAG-protein interaction is the role of Hp as an antithrombin III activator. A pentasaccharide unit with a very specific pattern of modification interacts with antithrombin III causing it to undergo a conformational change that increases the anticoagulation activity of antithrombin III by more than 3 orders of magnitude (7, 8). Contamination of pharmaceutical Hp was a major issue recently, *i.e.* associated with over 70 fatalities worldwide (9–12). This problem highlights the need for rapid, robust, and sensitive analytical methods for the analysis of heparin and for identifying contaminants of similar composition (11). Although nuclear magnetic resonance spectroscopy is often the method of choice for determining the structure of GAGs, such as Hp and HS, it requires substantial sample preparation to obtain pure samples, relatively large amounts of sample, and time-consuming interpretation.

Mass spectrometry (MS) and tandem mass spectrometry (MS/MS) offer high sensitivity and specificity and are often used for the analysis of complex mixtures. For these reasons, MS and MS/MS have been explored by a number of researchers as tools for the structural analysis of GAGs (13–31). Recently, the sequence of intact full-length chondroitin sulfate GAG chains from bikunin was elucidated (32). However, these were sparsely sulfated compared with typical HS/Hp GAGs, averaging less than 0.5 sulfate modifications per disaccharide repeat unit. Hp in particular is highly sulfated, making it extremely difficult to deduce composition and other structural details from intact samples. Controlled enzymatic digestion (heparin lyases I, II, and III) (33) and chemical methods (using nitrous acid) (34) can depolymerize Hp and HS to oligosaccharides of sizes that can be analyzed using the current

From the ‡Department of Chemistry, University of Georgia, Athens, Georgia 30602, the §Department of Chemistry and Chemical Biology, Chemical and Biological Engineering, and Biology, Rensselaer Polytechnic Institute, Troy, New York 12180, and the ¶Division of Chemical Biology and Medicinal Chemistry, Eshelman School of Pharmacy, University of North Carolina, Chapel Hill, North Carolina 27599

Received December 17, 2012, and in revised form, February 19, 2013

Published, MCP Papers in Press, February 21, 2013, DOI 10.1074/mcp.M112.026880

[1] The abbreviations used are: Hp, heparin; HS, heparan sulfate; GAG, glycosaminoglycan; IdoA, iduronic acid; dp, degree of polymerization; GlcA, gluconic acid.

instrumentation. The resulting products occur as a mixture of different sizes, compositions, isomers, and epimers, making their characterization extremely challenging.

Use of MS to analyze highly sulfated HS oligosaccharides, with two or more sulfo groups per disaccharide repeating unit, is difficult due to the loss of labile SO_3 with mild ion activation (27). Negative mode electrospray ionization (ESI) is commonly used to analyze GAGs due to its ability to preserve the sulfo groups during the ionization process and its propensity to form multiply charged anions from these acidic molecules (35). Information about the composition and the length of the molecule can be achieved by the first step MS but cannot provide structural details on the monosaccharide residue connectivity and locations of various GAG modifications, *i.e.* sulfo groups, acetyl groups, and uronic acid C_5 epimers. MS/MS is required to obtain these structural details. Fragmentation of glycosidic bonds produce ion products that determine the composition of individual residues, although cross-ring cleavages are useful for assigning the sites of modification within a monosaccharide residue.

For Hp and HS oligosaccharides, previous studies have shown that threshold ion activation methods such as low energy collision-induced dissociation (CID) or infrared multiphoton dissociation produce a relatively low number of structurally useful fragments, due to the preference for loss of SO_3 rather than glycosidic bond fragmentation or cross-ring cleavage (13, 25, 36). Nevertheless, CID has been used to differentiate 6-*O*-sulfo and 3-*O*-sulfo groups in Hp disaccharide units, due to differences in their multidimensional tandem mass spectrometry (MS^n) fragments (37). Metal cationization has also been used for the MS/MS analysis of carbohydrates (38–42), and it has been found that increasing the charge state and metal-hydrogen exchange in these biomolecules increases the density of fragments and reduces SO_3 loss (17, 25, 43, 44). Hp and HS GAGs have been characterized by their MS^n with CID activation, for both multiply charged ions cationized by Ca^{2+} (and Na^+ to a lesser extent), ranging from a trisaccharide with four sulfo groups to a pentasaccharide with eight sulfo groups. Although this work resulted in more glycosidic and cross-ring cleavages, there were still too few fragment ions to provide detailed structural information about the sites of sulfo group modifications (25). However, this work established that the presence of metal cations in these molecules increased the stability of the sulfo groups, leading to more useful fragment ions (45). In recent years, electron-based methods, especially electron detachment dissociation, have proved to be very useful in both locating the sulfo groups and determining the uronic acid C-5 stereochemistry of undersulfated HS-derived tetrasaccharides, but the efficiency of electron detachment dissociation decreases as the number of sulfo groups per disaccharide unit increases (13–16, 18, 20, 22).

Sodium metal cation/proton exchange has been investigated for electron detachment dissociation and infrared multiphoton dissociation of sparsely sulfated dermatan sulfate oligosaccharides (one sulfo group per disaccharide) (17). This work shows that increasing sodium cationization so that all sulfo groups in the molecule are deprotonated greatly reduces the number of peaks due to SO_3 loss, but this approach also resulted in a reduction of the number of both glycosidic and cross-ring cleavages (17). This study demonstrates a new method to stabilize sulfo groups during MS/MS of Hp and HS oligosaccharides, while producing much more extensive and structurally informative fragmentation. This is achieved by the exhaustive deprotonation of all ionizable sites in Hp and HS oligomers, using sodium hydroxide to cationize or deprotonate every acidic group in the precursor ion. This approach has recently been shown in our laboratory to be effective for the highly sulfated heparin-like pentasaccharide drug, Arixtra® (46). Here, we show that this approach is generally applicable to Hp and HS oligosaccharides from pentasulfated tetrasaccharides up to undecasulfated octasaccharide Hp, derived from natural sources, as well as chemoenzymatically synthesized HS oligomers up to 12 residues in length.

EXPERIMENTAL PROCEDURES

GAG oligomers were produced from naturally occurring sources and by chemoenzymatic synthesis. Those produced by enzymatic digestion of naturally occurring GAGs range from a pentasulfated tetrasaccharide to an undecasulfated octasaccharide. The chemoenzymatically synthesized oligosaccharides range from a decasaccharide with eight sulfo groups to a dodecasaccharide with 10 sulfo groups and under-sulfated HS ranging from degree of polymerization (dp) 10 to dp12.

Natural Hp Oligosaccharide Preparation—The heparin sodium salt used was obtained from porcine intestinal mucosa (Celsius Laboratories, Cincinnati, OH). Heparin (6 g) was digested with 10 units of recombinant heparinase 1 (EC 4.2.2.7) in a 250-ml volume at 30°C until 30% completion when boiling water was used to quench the reaction. Vacuum rotary evaporation was used to concentrate the reaction mixture before filtering with a 0.22-μm Millipore membrane. Before loading the filtrate into the P-10 (Bio-Rad) column, the column was equilibrated and eluted with 0.2 M NaCl solution. Uniform size oligosaccharide fractions were pooled together and then desalted using a P-2 column. These uniformly sized oligosaccharides were lyophilized and then purified on a semi-preparative strong anion exchange (SAX)-HPLC (Waters Spherisorb S5). Fractionation of various uniformly sized oligosaccharide mixtures was carried out using a gradient of water and 2 M NaCl, and chromatographic profiles at 232 nm were used to combine fractions from repeated separations. Primary structure and the level of purity were performed using PAGE analysis (47).

Chemoenzymatically Synthesized HS Preparation—A detailed procedure on the preparation of HS oligosaccharides used in this study can be found in Ref. 48. Briefly, *N*-sulfonation or 6-*O*-sulfonation was performed by incubating 6 μg of de-*N*-trifluoro-acetylated or de-6-*O*-sulfo *N*-trifluoro-acetylated oligosaccharide substrates with the appropriate enzymes and 3′-phosphoadenosine 5′-phosphosulfate, overnight at 37°C in a mixture of 80 μM 3′-phosphoadenosine 5′-phosphosulfate, 50 mM MES, pH 7.0, 1% Triton X-100, and 4 μg of *N*-sulfotransferase or 6-*O*-sulfotransferase-1 and 6-*O*-sulfotransferase-3 in a total volume of 300 μl. Purification was carried out using a DEAE column and dialyzed using 2500 molecular weight cutoff

(MWCO) 3500 membrane and dried before further purification by a DEAE-NPR HPLC column (0.46 × 7.5 cm; TosoHaas) (48).

Mass Spectrometry Analysis—A 9.4 Bruker Apex Ultra Qh-FTICR instrument (Billerica, MA) was used in these experiments. Negative mode ESI was used to ionize the samples using a metal capillary (G2427A, Agilent Technologies, Santa Clara, CA). The samples were introduced at a concentration 0.05–0.1 mg/ml in 50:50 methanol/H_2O. The degree of sodiation was controlled by the addition of 1–2 mM NaOH (Sigma-Aldrich) to the electrospray solution depending on the level of sulfation of the analyte. All samples were infused at the rate of 120 μl/h. The precursor ions were mass isolated in the external quadruple with a 3-Da isolation window, and CID was performed in the collision cell external to the high magnetic field region while ensuring the precursor ion intensity remained above the product ion intensity to minimize the production of internal fragments. The effect of adding NaOH in the solution was studied by first introducing the sample in H_2O/MeOH only and then with NaOH to a hexasaccharide containing eight sulfo groups. The MS of the hexasaccharide sample with and without NaOH is shown in the supplemental Fig. S1. Molecular ions of charge state envelope for 3−, 4−, 5−, and −6 were observed. Within the charge state envelope, there are numerous peaks resulting from metal/hydrogen exchange. These include the ones with Na^+ and K^+/H^+ individually and the ones with a combination of Na^+ and K^+ in a single peak. This phenomenon is clearly seen when we zoom in one charge state envelope as shown in supplemental Fig. S1. The zoom in of the 5^- charge state shows the distribution of metal cation/hydrogen exchange peaks. One striking observation from these data is the disappearance of K^+ and Na^+/K^+ peaks after the addition of 1 mM NaOH solution. The peak intensities of the remaining Na^+ peaks increase 2-fold, enabling the isolation of the precursor in the quadruple mass filter without interfering peaks around that would otherwise be co-isolated with the precursor.

One megapoint of data was acquired for each mass spectrum, padded with one zero-fill, and apodized using a sine bell window. A 5-ppm mass accuracy was achieved through an external calibration, and internal calibration using accurately assigned glycosidic bond cleavage products yields a mass accuracy of <1 ppm. Accurate mass measurement values were used to assign product ions, whose *m/z* values were calculated using GlycoWorkbench version 2.1 (49). The product ions are reported using the annotation described previously (18), derived from the Domon and Costello nomenclature (50).

RESULTS AND DISCUSSION

Negative-mode ESI is a useful method for analyzing highly sulfated GAGs because the labile sulfo groups are retained and also because multiply charged anions are produced (5). Sulfo and carboxyl groups comprise the acidic groups in GAGs, which serve as charge-bearing residues in the ionized sample. Alkali ion/proton heterogeneity can be a significant issue for highly sulfated GAGs, because a substantial reduction in ion intensity results when the signal is divided into several different mass channels. Adding formic acid to the sample solution reduces both Na^+ and K^+ heterogeneity in less sulfated GAGs, but it is less efficient for longer and more highly sulfated Hp and HS oligosaccharides. Although formic acid reduces the intensity of the Na^+ and K^+ peaks, they are still present, leading to difficulties during the ion isolation step of a tandem mass spectrometry experiment; there can be many co-isolated peaks that complicate the resulting MS/MS spectrum. As shown in the supplemental material, addition of 1 mM NaOH removes all the adduct peaks that contain K^+, retaining only Na^+ adducts. This increased the signal intensity of the remaining Na^+ containing peaks and allowed clean selection of the precursor ions by the mass selective quadruple. The structures of all the GAG molecules used in this work can be found in supplemental Fig. S2. Also found in the supplemental material are their mass spectra showing the molecular ions obtained and an inset of an expansion of regions around the precursor ions used in the MS/MS analysis.

A pentasulfated tetrasaccharide (ΔUA2S-GlcNS6S-GlcA-GlcNS6S) (T1) was examined using the procedures described above. The mass spectrum of this compound produced 2−, 3−, and 4− charge state molecular ions as shown in the supplemental material. One of the molecular ion $[M - 7H + 4Na]^{3-}$ that was selected for CID analysis has all the acidic groups ionized, including five sulfo and two carboxyl groups. A simple spectrum was obtained in which the fragment ions permit the identification and location of all the sulfo groups (Fig. 1). All the observed fragment ions are either singly or doubly charged. The three most intense peaks in the spectrum are cross-ring fragments $[^{0,2}A_4 + 4Na]^{2-}$, and a fragment from the same fragment with water loss, and $[^{2,4}A_4 + 4Na]^-$. The fragmentation pathway for these $^{0,2}A_n$ and $^{2,4}A_n$ fragments at the reducing end is highly favored, and they are observed as the most intense fragments in all the highly sulfated compounds with two sulfo groups in the reducing end residues and from a precursor with all the acidic groups de-protonated. Abundant $^{0,2}A_n$ fragmentation on the reducing end has been observed for CID of heparin disaccharides by others and the mechanism for its occurrence postulated by a reducing end retro-aldol rearrangement pathway (30, 51, 52). $^{0,2}A_n$ formed at the reducing end can undergo further fragmentation forming $^{2,4}A_n$ product ion (53), and this may explain the appearance of intense $^{2,4}A_n$ fragments within the reducing end of the aldehyde-terminated molecules studied here. CID fragmentation of the same fully deprotonated precursor ion $[M - 7H + 4Na]^{3-}$ from an isomeric tetrasaccharide (T3) (discussed below) without sulfation at the 6-*O*-position on the reducing end preceded by 2-*O*-sulfated IdoA produced much less intense $[^{2,4}A_4 + 4Na]^{2-}$, an indication that the presence of 6-*O*-sulfation at the reducing end amino sugar promotes the occurrence of this fragment. Additionally, the CID spectra for the T3 $[M - 7H + 4Na]^{3-}$ precursor had a markedly higher percentage of SO_3 loss (2% of the fragment ion intensity) compared with a much lower degree of SO_3 loss for the T1 (<1%) as indicated in Table I. Other observable MS/MS spectral differences between these precursor ions for the two isomers can be obtained in the supplemental material. The location of the two sulfo groups in the reducing end residue T1 are identified by the $^{2,4}X_0$ peak or by the mass difference between the $^{2,4}A_4$ and C_3 fragments. The location of the two sulfo groups in the central glucosamine residue derive from the mass difference between $^{2,4}A_2$ and B_2, whereas the site of sulfo group substitution in the nonreducing end residue is

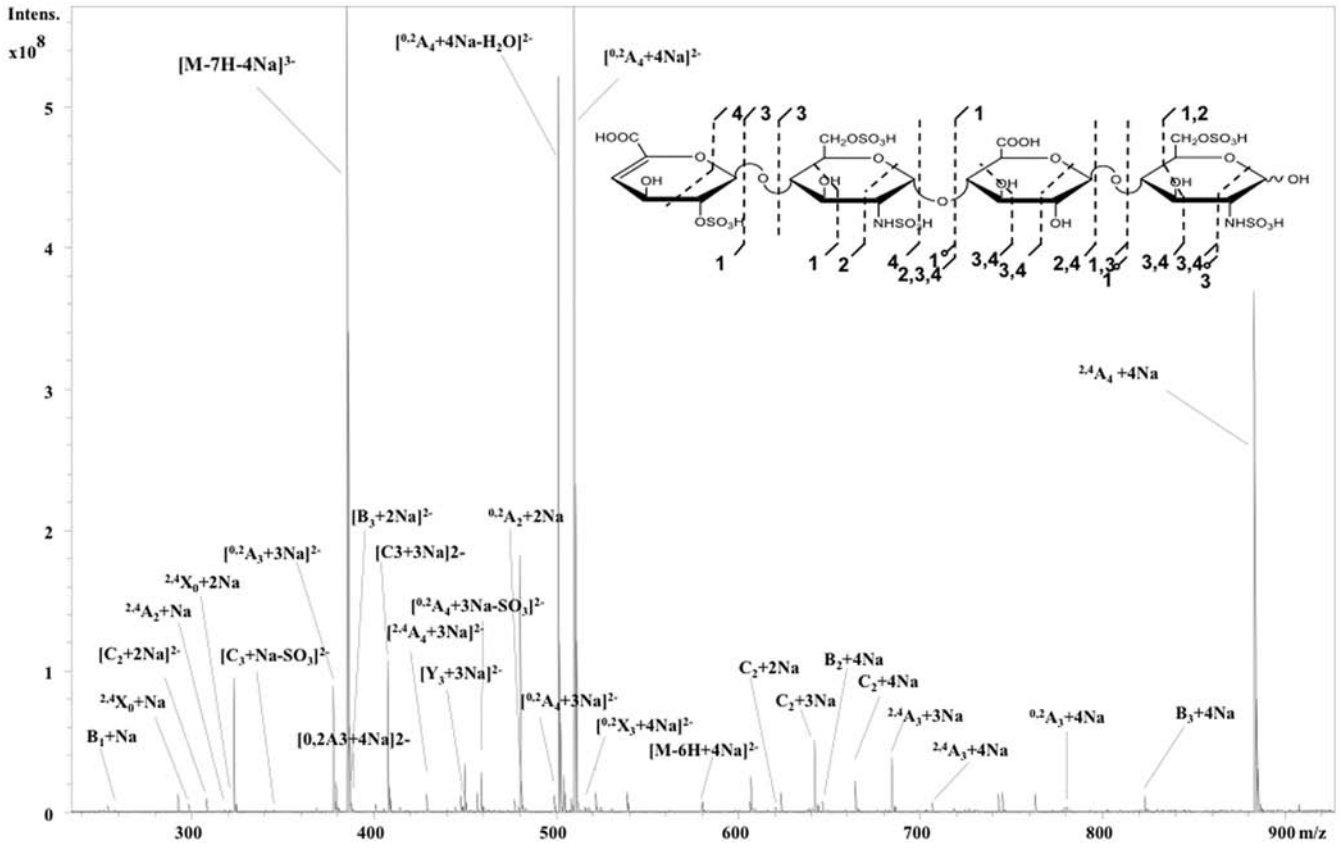

FIG. 1. **CID spectra of pentasulfated heparin tetramer, precursor [M − 7H + 4Na]$^{3-}$.** The fragment ions observed are shown in the annotated structure (*inset*). The precursor used has all the sulfates and carboxyl groups ionized through charge or Na^+/H^+ exchange.

TABLE I

Shown are the compounds and the precursor ions used in this work

The product ion yield is given by (the sum of all assigned product ions divided by the sum of all the ions in the spectrum including the precursor)·100. The percent of SO_3 loss experienced during the CID of the given precursor is calculated by summing up all the intensities of the fragments resulting from SO_3 loss and dividing this value with the sum of the intensities of all assigned fragment ions excluding the precursor and then multiplying the result by 100. Number of free protons in this work is calculated using this formula ((number of SO_3 + carboxyl groups in the compound) − (precursor charge + number of Na^+ in it)).

Compound, no. of sulfates, and precursor with its *m/z*	% product ion yield	% of SO_3 loss product ions	No. of free protons	Sulfate/disaccharide
dp4 (T1) 5S, $[M - 7H + 4Na]^{3-}$ *m/z* 386.29	54	<1	0	2.5
dp4 (T3) 5S, $[M - 7H + 4Na]^{3-}$ *m/z* 386.29	42	2	0	2.5
dp4 (T1) 5S, $[M - 6H + 2Na]^{4-}$ *m/z* 278.48	41	10	1	2.5
dp4 (T3) 5S, $[M - 6H + 2Na]^{4-}$ *m/z* 278.48	30	21	1	2.5
dp4 (T2) 6S, $[M - 7H + 3Na]^{4-}$ *m/z* 303.96	43	12	1	3
dp6 8S, $[M - 11H + 7Na]^{4-}$ *m/z* 450.20	55	1	0	2.7
dp8 11S, $[M - 14H + 7Na]^{7-}$ *m/z* 339.25	56	23	1	2.8
dp10 8S, $[M - 13H + 7Na]^{6-}$ *m/z* 412.66	44	11	0	1.6
dp7 7S, $[M - 10H + 5Na]^{5-}$ *m/z* 376.39	50	15	0	2
dp12 10S, $[M - 16H + 9Na]^{7-}$ *m/z* 430.85	41	14	0	1.7
dp12 5S, $[M - 11H + 4Na]^{7-}$ *m/z* 358.03	62	7	0	0.8
dp11 5S, $[M - 9H + 3Na]^{6-}$ *m/z* 384.87	62	7	1	0.9
dp10 4S, $[M - 9H + 3Na]^{6-}$ *m/z* 344.70	63	6	0	0.8

ascertained through the mass difference of $^{0,2}X_3$ and Y_3 fragments. The product yield from this precursor was 54%, and most of the remaining ion abundance was from the precursor ion whose intensity was considerably larger than the product ions (commonly observed in most of the mass spectra reported in this work even though product ion yields are 30–

60%, as product ions are divided between my fragment channels). There were only three peaks exhibiting SO_3 loss (from C_2, C_3, and $^{0,2}A_4$ fragments) accounting for less than 1% of the product ions confirming that the Na^+ ions stabilize the sulfo groups during ion activation leading to backbone fragmentations. CID of a precursor ion from the same compound, but with one ionizable proton present, $[M - 6H + 2Na]^{4-}$, also produced fragments that enabled the location of all sulfo groups in the molecule but with markedly increased SO_3 loss.

This approach was tested with two additional tetrasaccharides ΔUA2S-GlcNS6S-IdoA2S-GlcNS (T3) and ΔUA2S-GlcNS6S-IdoA2S-GlcNS6S (T2), with five and six sulfo groups, respectively. CID for singly protonated molecular ions for T2 $[M - 7H + 3Na]^{4-}$ and T3 $[M - 6H + 2Na]^{4-}$ produced fragments that were able to locate all sites of sulfo group substitution. The structures for T2 and T3 with annotations denoting the sites of observed fragmentation as well as their MS/MS spectra and tables with the *m/z* values and assignment of the fragments can be found in the supplemental material. A lower charge state molecular ion $[M - 7H + 4Na]^{3-}$ for T3 produced a product yield of 42% with only a total of 21 fragment ions in the spectrum with 2% of all the products resulting from SO_3 loss. CID of T2 molecular ion $[M - 8H + 5Na]^{3-}$ produced only 12 fragments (six cross-ring and six glycosidic) with no loss of SO_3 fragments observed. Another observation is that the presence of an acidic proton in the selected precursor within these tetrasaccharide units leads to much higher SO_3 loss, as seen from Table I. T1 precursor $[M - 7H + 4Na]^{3-}$ with no free proton show less than 1% SO_3 loss, whereas a different precursor $[M - 6H + 2Na]^{4-}$ of the same compound but with a free acidic group produced 10% SO_3 loss (the same is observed for T3).

An interesting observation from these data was the correlation of particular fragment ions with uronic acid stereochemistry. $^{2,4}A_n$ appears with significant abundance in the glucuronic acid residue and is absent or present at very low abundance in 2-*O*-sulfated iduronic acid residues. As will be seen in the data below, $^{2,4}A_n$ cleavages are absent in 2-*O*-sulfated iduronic acid residues for all the compounds that we have analyzed, except in these tetrasaccharides, where they may occur with low abundance. These suggest that these ions may be used to assign the stereochemistry of the uronic acid residues in Hp and HS oligosaccharides. Because the analyzed compounds do not contain desulfated uronic acid residues, further investigations are required to ascertain whether the observed fragmentation pattern is due to the presence of the sulfate group in the iduronic acid, and this is currently being done by exploring heparin and heparan sulfate analytes containing desulfated uronic acid residues. Ongoing work using this approach on epimeric chondroitin and dermatan sulfate dp4–10 oligosaccharides containing GlcA and IdoA, which are not sulfated, indicate that the $^{2,4}A_n$ fragment often appears exclusively in GlcA and is absent in IdoA residues indicating that it may be useful in assigning the uronic acid stereochemistry in those kinds of GAGs.[2]

The octasulfated hexasaccharide (ΔUA2S-GlcNS6S-IdoA2S-GlcNS6S-GlcA-GlcNS6S) was examined by this method, and its CID spectrum is shown in Fig. 2. The mass spectrum obtained from this compound contained charge states 3−, 4−, 5−, and 6− as can be seen in the supplemental material. Like the tetrasaccharides, the precursor ion selected for analysis, $[M - 11H + 7Na]^{4-}$, had all 11 acidic groups deprotonated. The fragment ions $[^{2,4}A_6 + 7Na]^{2-}$, $[^{0,2}A_6 + 7Na]^{3-}$, and its water loss are found to produce the three most intense peaks in this spectra, similar to the tetrasaccharide in Fig. 1. Despite the density of the sulfates per disaccharide (2.7), total ion current of SO_3 loss fragments resulting from the CID of this fully deprotonated precursor was 1% of the total ion abundance, excluding the precursor intensity (Table I). As it can be seen from Fig. 3, there are more X, Y, and Z fragments on the nonreducing side of the molecule and more A, B, and C fragments on the reducing end side, whereas the middle residues of the molecule exhibit only a few fragments. However, the abundant glycosidic and cross-ring fragment ions obtained unambiguously locate all the sulfo groups in the compound except for the one in the iduronic acid (third residue from the nonreducing end). This modification could be located using a different precursor $[M - 11H + 6Na]^{5-}$ (data not shown).

The undecasulfated octasaccharide (ΔUA2S-GlcNS6S-IdoA2S-GlcNS6S-IdoA2S-GlcNS6S-GlcA-GlcNS6S) was successfully characterized by this method (Fig. 3). There are 11 sulfo and four carboxyl groups in this octasaccharide, corresponding to 15 ionizable protons. The $[M - 14H + 7Na]^{7-}$ ion with a single protonated acidic group was analyzed by MS/MS. Multiple molecular ions for charge states 4−, 5−, 6−, and 7− were observed in the mass spectrum of this compound. Use of 2 mM NaOH for this long and densely sulfated oligomer led to the reduction of less sulfated molecular ions leaving only highly sodiated ones. The mass spectrum and the expanded regions of the precursor ion used for CID analysis can be obtained from the supplemental material. An interesting observation made during the application of this approach for highly sulfated compounds is that it gets harder to get fully deprotonated molecular ions at higher charge states. For this dp8, there was no fully deprotonated molecular ion $[M - 15H + 8Na]^{7-}$ observed in the MS spectrum, but other fully deprotonated precursor ions appeared in all other charge states with increasing intensity as the charge state decreased. This observation was also partly true for the dp4 and dp6 compounds analyzed as can be seen in the supplemental material.

The three most intense fragments observed in the tetrasaccharide and hexasaccharide samples above were absent or of low intensity. The reducing end $^{0,2}A_8$ fragment was

[2] M. J. Kailemia, A. B. Patel, D. T. Johnson, L. Li, R. J. Linhardt, I. J. Amster, manuscript in preparation.

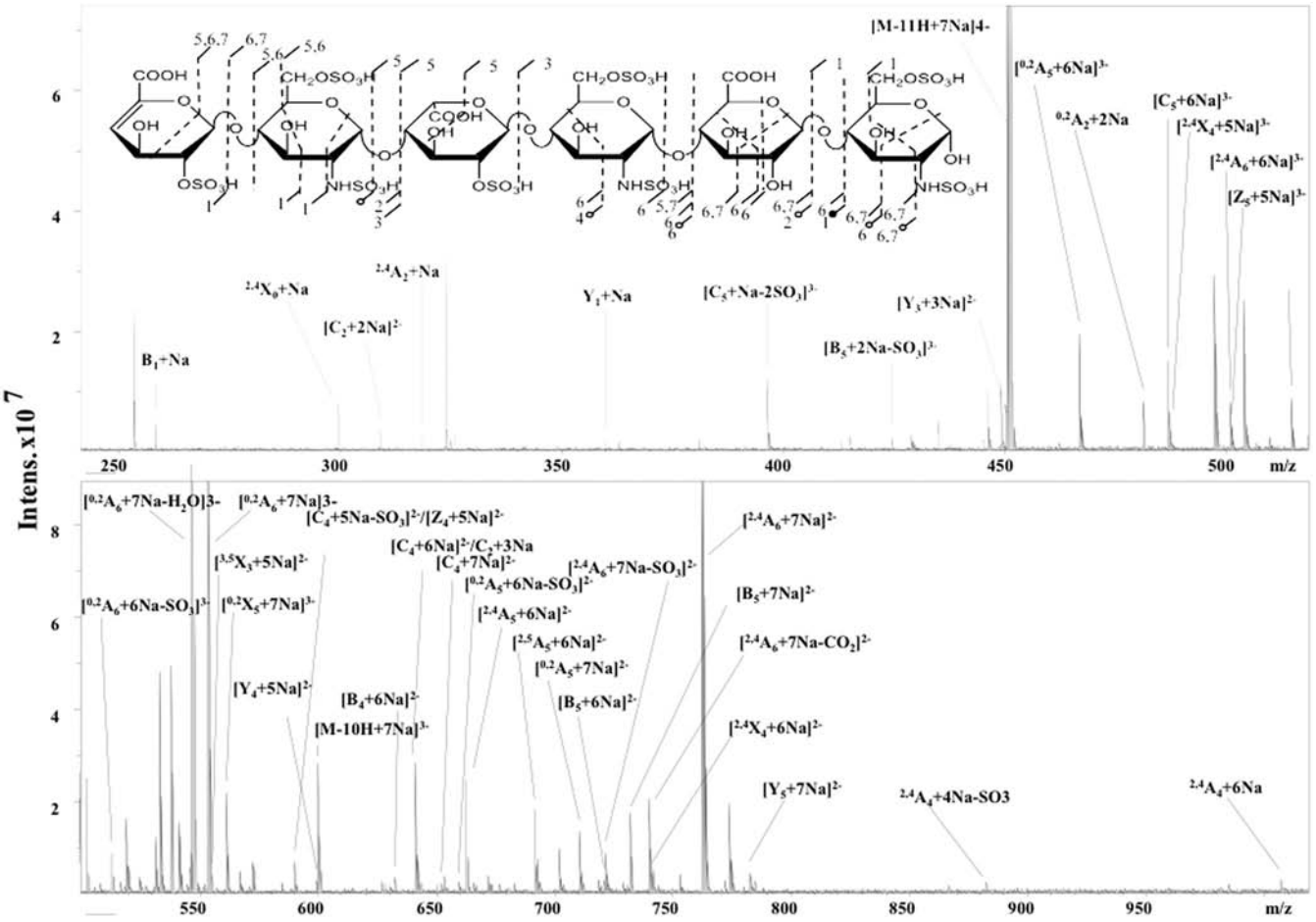

FIG. 2. **CID spectrum of the precursor $[M - 11H + Na]^{4-}$ for the hexamer with eight sulfate and three carboxylate groups.** All the acidic groups in this precursor are ionized, and the annotated structure is shown in the *inset*. Abundant glycosidic and cross-ring cleavages enable the location of the sulfate modifications in the structure.

observed but in low intensity, and there was no $^{2,4}A_8$ product ion observed, which is an indication that the presence of a free acidic proton within the ion has a profound effect on the fragments observed at the reducing end residue especially the $^{2,4}A_n$ fragments. Increased loss of SO_3 was observed accounting for 23% of the total ion abundance (Table I). We believe that the mobile acidic proton as well as the density of the sulfates (2.8 sulfates per disaccharide) within this dp8 oligomer has a substantive contribution to the observed increase in SO_3 loss. Despite this increase in SO_3 loss, the product yield was high (56%), and there were sufficient glycosidic and cross-ring fragments to locate all the sulfo groups except the one on the reducing end residue, which was established after fragmenting the fully deprotonated precursor $[M - 15H + 9Na]^{6-}$, and one in the iduronic acid residue (4th from the nonreducing end). As observed in those other heparin oligosaccharides analyzed above, the charge-reduced precursor $[M - 13H + 7Na]^{6-}$ was present in high abundance in the CID spectra of the analyzed precursor.

Part of the challenge in structural elucidation of highly sulfated GAGs using mass spectrometry is the lack of structurally defined oligosaccharides. A complementary method to chemical synthesis that generates well defined HS structures is the use of regioselective HS biosynthetic enzymes to synthesize structurally defined sulfated oligosaccharides. Tandem mass spectrometry of these compounds can help to build a library of well defined fragments from specified structures that can be useful in identifying unknowns. This work shows the analysis of this type of oligosaccharide using CID, and the results establish the capability of this approach to locate the sites of sulfo group substitution in most oligosaccharides.

Fig. 4 shows the chemoenzymatically synthesized heptasaccharide, GlcNAc6S-GlcA-GlcNS3S6S-IdoA2S-GlcNS6S-GlcA-AnMan, with seven sulfo groups and three carboxyl groups. This molecule is similar in structure to the drug, Arixtra®, which was examined recently using this approach (46). The differences in structure from the chemoenzymatically produced compound are that the first two residues from the reducing end are replaced by a methyl group in Arixtra®, and the nonreducing end residue contains an *N*-sulfo group in Arixtra®, but an *N*-acetyl group in the chemoenzymatically

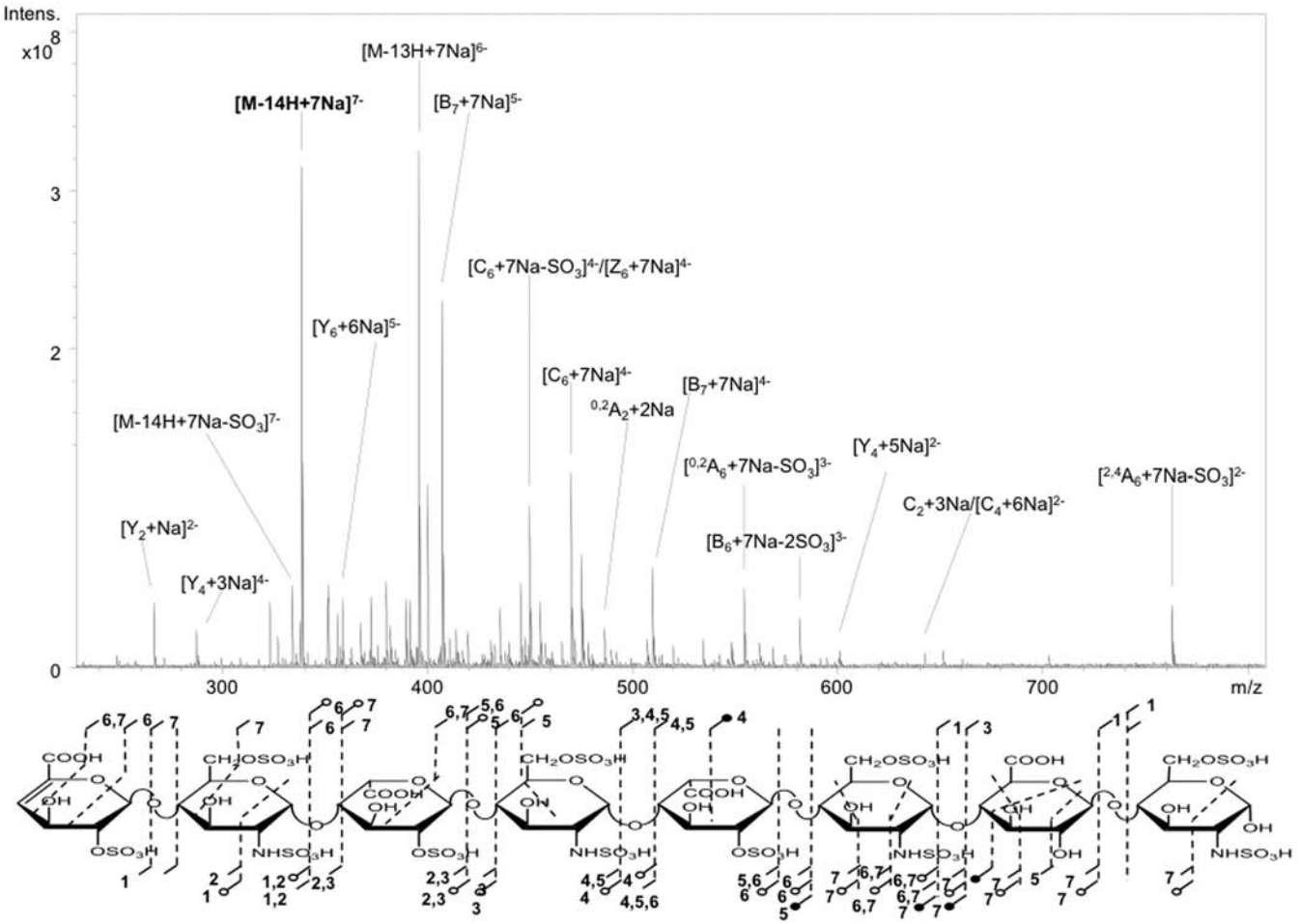

FIG. 3. **CID spectrum for an octamer with 11 sulfates.** The precursor $[M - 14H + Na]^{7-}$ used had only one acidic group uncharged. Because of the density of ions formed, only the most intense fragments are annotated. Full assignment of all the fragments is placed in the supplemental material. The annotated structure showing the fragments obtained is located *below* the spectrum.

prepared compound. The spectrum obtained from a fully deprotonated molecular ion $[M - 10H + 5Na]^{5-}$ produced abundant glycosidic and cross-ring fragments that are able to locate all the sulfo groups in the molecule, including the trisulfated saccharide residue (third from the nonreducing end). Because there are only three possible sulfo group locations in this residue, the mass difference from glycosidic bond fragments Y_5 andY_4 provides sufficient information to locate them. 15% of the product ion intensity was due to SO_3 loss. This is understandable considering the density of the SO_3 per disaccharide which is two and the presence of a trisulfated amino sugar within the chain (Table I).

The presence of 3-*O*-sulfation in the trisulfated residue seems to affect its fragmentation patterns. Unlike most of the other amino sugar residues, ^{0,2}A and ^{2,4}A fragments are absent in the trisulfated sugar residue in the obtained CID spectra of this heptasaccharide, and similar behavior was apparent during the analysis of Arixtra®, which also contains a trisulfated amino residue. Researchers have postulated earlier that a C_n glycosidic fragment can undergo further fragmentation to form ^{0,2}A ion, which can in turn lead to the formation of ^{2,4}A ion within 1–4-linked glycans (52, 53). The fragmentation mechanism for the formation of the ^{0,2}A ion requires the 3-*O*-hydrogen in the sugar ring (30), and because the 3-*O*-hydrogen is substituted with SO_3 group within the trisulfated residue, this fragmentation pathway may be less favored. As noted earlier, $^{2,4}A_n$ fragments are common in glucuronic acid residues and extremely rare in 2-*O*-sulfated iduronic acid monosaccharides. There are two glucuronic acid residues and one 2-*O*-sulfated iduronic acid residue present in this oligosaccharide. The $^{2,4}A_n$ fragments are only present in the two glucuronic acid residues and none on the 2-*O*-sulfated iduronic acid residue.

The tandem mass spectrum of a chemoenzymatically produced decasaccharide with eight sulfo groups (GlcA-(GlcNS6S-GlcA)$_4$-AnMan) is shown in Fig. 5. Molecular ions having charge state 5^-, 6^-, and 7^- were obtained in the mass spectrum for this compound, and the molecular ion $[M - 13H + 7Na]^{6-}$ was used for CID analysis (supplemental material). All the sulfo groups in the decasaccharide can be unambiguously

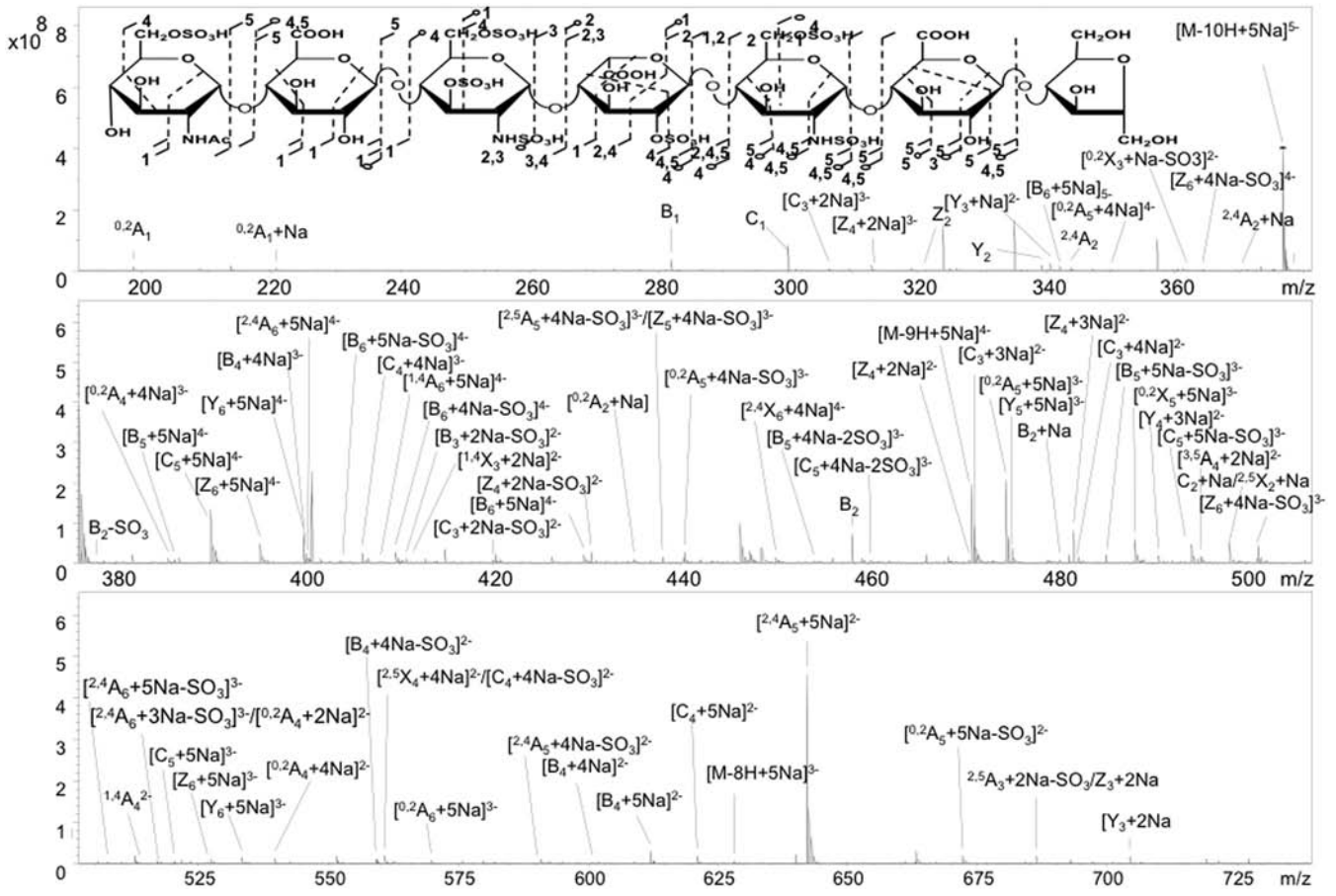

FIG. 4. **CID spectrum of heparin heptasaccharide precursor [M − 10H + 5Na]$^{5-}$ with all the acidic groups deprotonated.** Abundant glycosidic and cross-ring cleavages provide sufficient information to determine the location of all the sites of sulfation. *Inset* is the annotated structure showing the obtained fragments.

located except the one on the 2nd residue from the nonreducing end. Because of the large number of fragments obtained, only the most intense ones are annotated in the figure, but the entire annotations for this analyte can be found in the supplemental material. There are very few C and Z ions in the spectrum as compared with the B and Y ions. This is somewhat different for the highly sulfated oligosaccharides obtained from natural sources as discussed above. The most intense fragment ions from fully deprotonated molecular ions for the naturally occurring compounds analyzed here are the ^{0,2}A and ^{2,4}A ions at the reducing end residue, and the same type of ions appears to dominate this spectrum and the one for dp7 (discussed above), but this time they appear in the disulfated amino sugar, the third residue from the reducing end of these molecules. One characteristic for these intense daughter ions for all the samples tested using this method is that they appear when a fully deprotonated precursor is fragmented, and these daughter ions themselves contain fully deprotonated acidic groups. The result obtained for the dodecasaccharide with 10 sulfo groups (GlcA-(GlcNS6S-GlcA)$_5$-AnMan), whose MS/MS spectrum and annotated peak list are found in the supplemental material, is similar to that of dp10 discussed above. Most of the sulfo groups were located after fragmenting the full deprotonated precursor, [M − 16H + 9Na]$^{7-}$. The fragmentation due to the SO_3 loss for the dp10–8S and dp12–10S accounted for 11 and 14% of the total ion abundance, respectively, as shown in Table I, consistent with the number of sulfate groups in the analyzed chain.

Fig. 6 shows a CID spectrum acquired from a fully deprotonated precursor ion, [M − 11H + 4Na]$^{7-}$, of dodecasaccharide (GlcA-(GlcNS-GlcA)$_5$-AnMan) with five sulfo groups. In the MS spectra charge states 4−, 5−, 6−, and 7− were observed (supplemental material). Although only the most abundant fragment ions are annotated in Fig. 6, most of the low intensity fragments could be assigned, as can be seen in the *inset*, representing an expansion of the region *m/z* 460–500. All other annotations from this compound are listed in the supplemental material. It is noteworthy that the product yield was high (62%), and the most intense fragments were either glycosidic or cross-ring fragments and not fragment ions resulting from SO_3 loss, which accounted for only 7% of the total product ion intensity. All the sulfo groups were located unambiguously.

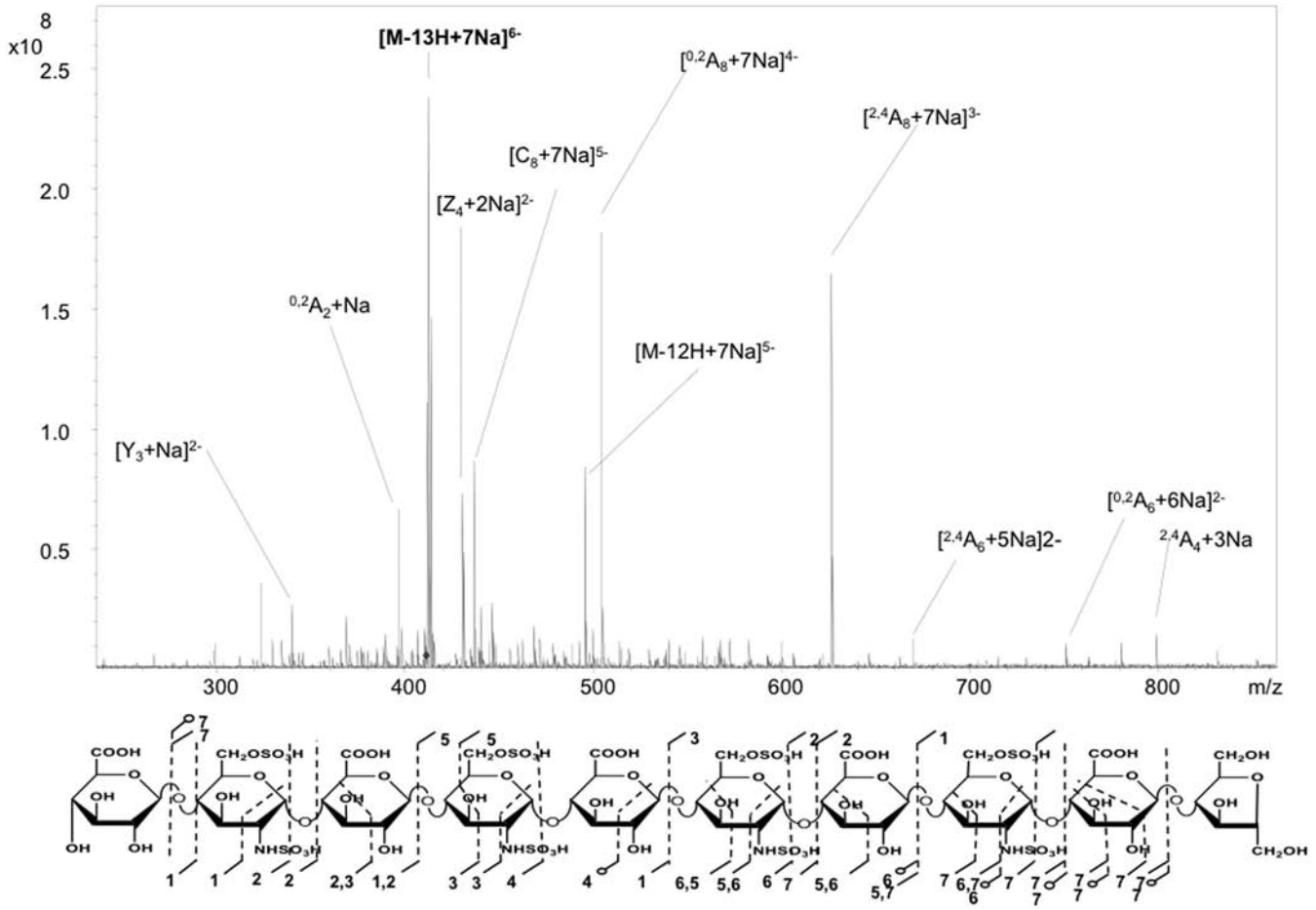

FIG. 5. **Shown are [M − 13H + 7Na]$^{6-}$ CID spectrum and the annotated structure for highly sulfated HS decasaccharide.** Only the most intense fragments are annotated, but all the ion assignments can be found in the supplemental material. *Below* the spectrum is the annotated structure showing the fragments obtained.

The annotated structures for a decasaccharide (GlcA-(GlcNS-GlcA)$_4$-AnMan) and an undecasaccharide ((GlcNS-GlcA)$_5$-AnMan) with four and five sulfo groups, respectively, are shown in Fig. 7. A fully deprotonated precursor was used to obtain the data that assigned the sulfo group positions for dp10. Because of a low density of fragments obtained from the fully deprotonated precursor for dp11 (data not shown), a precursor with one protonated acidic group was used. A large number of both glycosidic and cross-ring fragments enabled the assignment of the location of all the sulfo groups for the decasaccharide structure except the sulfo group in the second residue from the nonreducing end, which can be easily identified after fragmenting a singly protonated acidic group precursor for the same charge state. The sites of sulfo group substitution in the dp11 were all located except the one at the nonreducing end. Just like the more highly sulfated chemoenzymatically synthesized GAGs studied above, there were very few C and Z ions observed in these spectra. As expected, the less sulfated chemoenzymatically GAGs (0.8–0.9 sulfates/disaccharide) had very low levels of SO_3 loss (6–7%), and the level is half of that observed for the same length but higher sulfated counterparts (1.6–1.7 SO_3/disaccharide). The presence of a free acidic proton in dp11 with five sulfates did not seem to affect this level as much as observed in the highly sulfated naturally produced GAGs (Table I). Additionally, the product yield for the less sulfated chemoenzymatically produced compounds (62–63%) was higher than the highly sulfated counterparts (41–50%) partly due to the relatively higher number of fragments that could not be assigned.

There were no cross-ring fragments obtained within the reducing end (AnMan) and the nonreducing end, as observed for all the chemoenzymatically produced oligosaccharides. This could be due to the type of residues in both the reducing end and the nonreducing end of these molecules. Unlike the chemoenzymatically produced GAGs used in this work, the naturally occurring heparin oligosaccharides analyzed contain Δ^{4-5}-unsaturated uronic acid at the nonreducing end, which promotes the formation of ^{0,2}X through the well established retro-Diels Alder rearrangement of the nonreducing end (30). The ^{0,2}X within the nonreducing end residue is observed in all the naturally occurring heparin oligosaccharides analyzed (Figs. 1–4) and not in any of the chemoenzymatic ones (Figs.

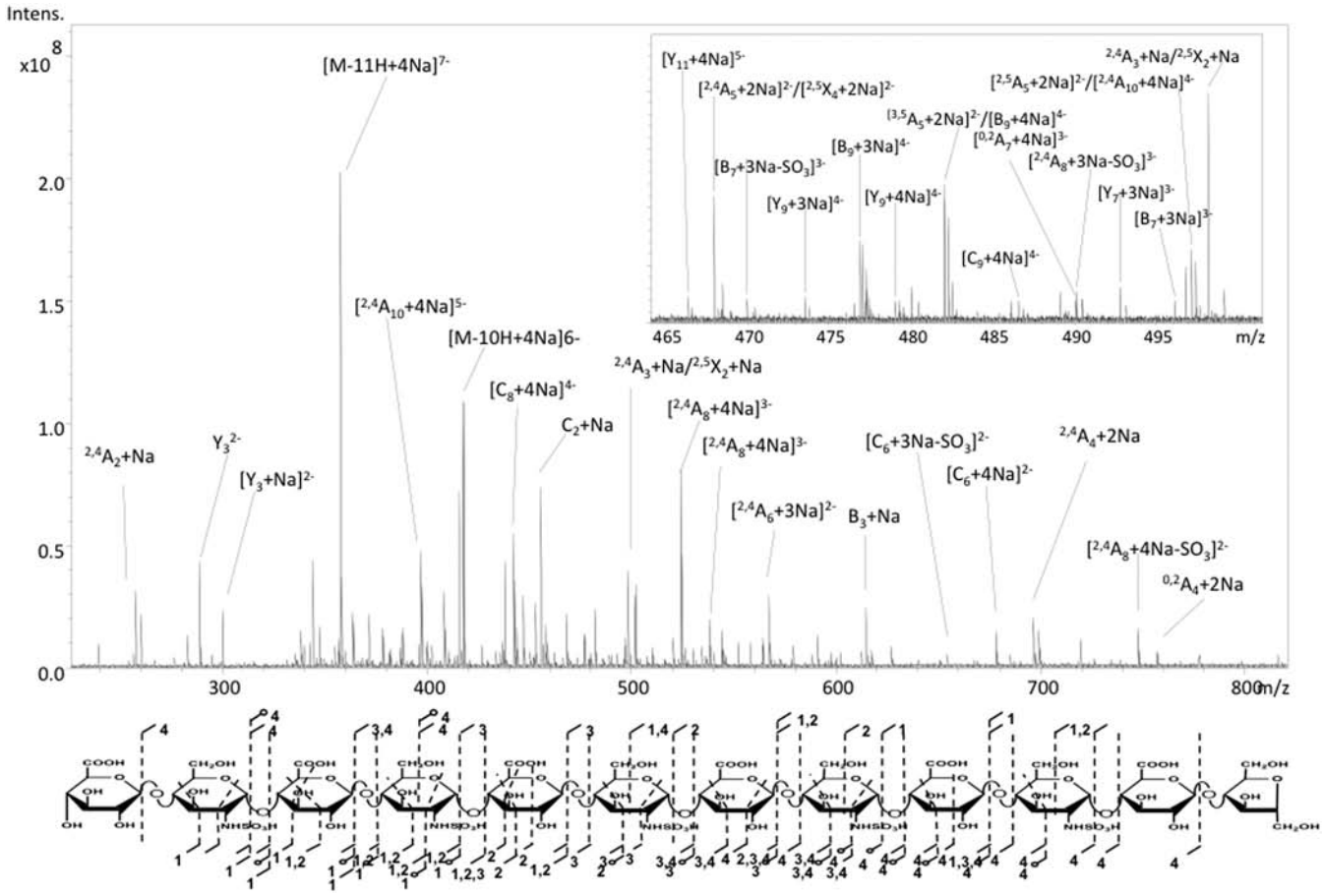

FIG. 6. **CID spectrum of chemoenzymatically produced dodecasaccharide precursor [M − 11H + 4Na]$^{7-}$ with the *inset* showing a small zoomed in region of the spectrum with the annotations.** Only the intense peaks are annotated, but all fragment assignments for this analyte can be found in the supplemental material.

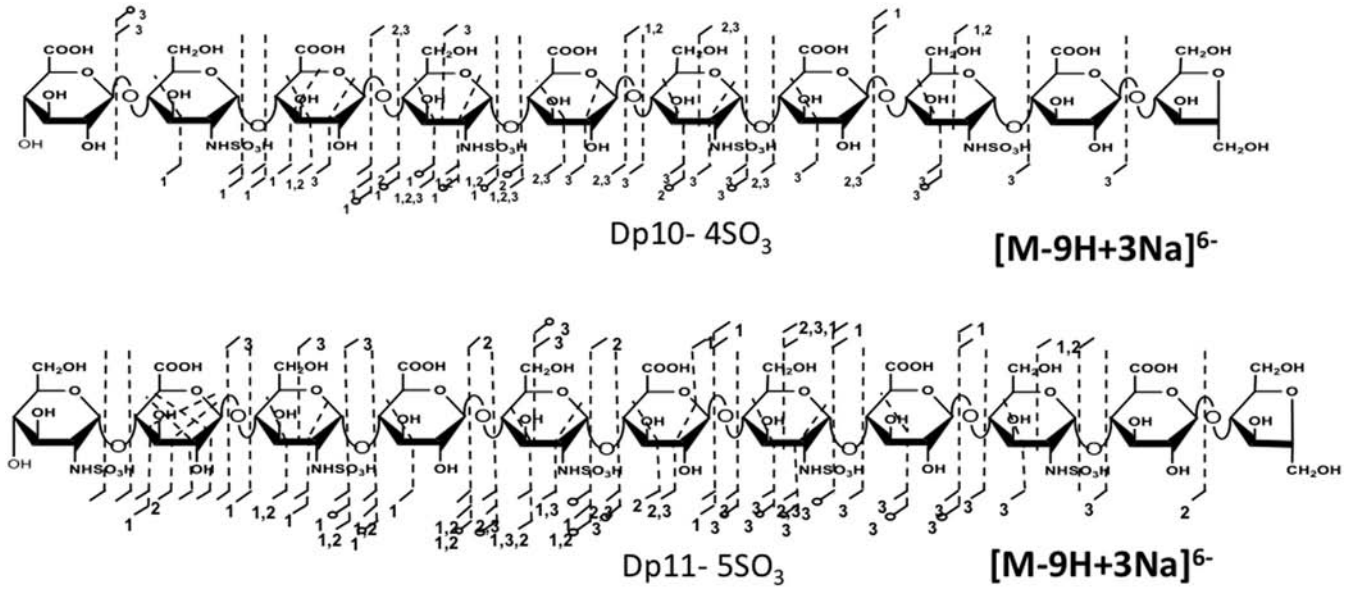

FIG. 7. **Annotated structures for dp10 and dp11 with four and five sulfates, respectively, showing the fragments obtained from the tandem mass spectrometry experiments.** The spectra for these compounds can be found in the supplemental material.

5–7). The disappearance of reducing end fragments observed in the naturally occurring heparins (Figs. 1–4) within all the chemoenzymatically produced GAGs (Figs. 5–7) tested by using this approach may be due to the lack of terminal aldehyde, which could promote the formation of the ^{0,2}A fragment through the retro-aldo rearrangement of the reducing end as noted above.

CONCLUSIONS

Although mass spectral analysis is widely used in proteomics, the mass spectrometric analysis of sulfated oligosaccharides has proven much more challenging, slowing the development of glycomics. This work demonstrates that under proper spray conditions, and with selection of the proper precursor, MS/MS using CID will yield a complete set of cross-ring and glycosidic fragment ions, which enables the characterization of highly sulfated Hp and HS oligosaccharides. The method is equally efficient for undersulfated and highly sulfated oligosaccharides as well as short and long Hp and HS chains. Useful structural information is produced when all the acidic groups are either deprotonated or undergo Na^+/H^+ exchange. Previous MS/MS studies on Hp and HS suggested that the charge state should be equal to or slightly more than the number of sulfo groups (21). This normally works well for shorter or more sparsely sulfated GAGs (zero to two sulfo groups per disaccharide subunit) but fails for highly sulfated GAGs (two to three sulfo groups per disaccharide subunit). Although other work had suggested use of ammonium acetate to improve upon Na^+ cationization, we find a substantial advantage from the addition of 1–2 mM NaOH to the spray solution, specifically the elimination of other interfering metal adducts, improving isolation and producing cleaner and easier to assign fragmentation spectra.

There is a difference between these results and those obtained previously with Ca^{2+} cationization, for which there were fewer useful fragments obtained for metal-adducted highly sulfated GAGs (25). In this previous study, Ca^{2+} adduction gave an improvement in the production of structurally significant product ions compared with those from precursors lacking metal cations. However, the precursors in prior studies were not exhaustively deprotonated. In all the compounds studied in this work, the precursor ions used had all acidic groups deprotonated or had one proton present. In most cases, a single precursor provides all the structural information (monosaccharide composition and the sites of sulfo group substitutions), but in few cases, a combination of assignments from fully deprotonated and from a singly protonated acidic group provided the full structural characterization. The work here demonstrates that this approach, recently demonstrated in our laboratory for the pentasaccharide drug Arixtra® (46), is generally applicable to Hp and HS oligomers of a broad range of lengths and degrees of sulfation.

* This work was supported, in whole or in part, by National Institutes of Health Grant 2R01-GM038060-20.

S This article contains supplemental material.

‖ To whom correspondence should be addressed. Tel.: 706-542-2001; Fax: 706-542-9454; E-mail: jamster@uga.edu.

REFERENCES

1. Capila, I., and Linhardt, R. J. (2002) Heparin-protein interactions. *Angew. Chem. Int. Ed. Engl.* **41,** 391–412
2. Casu, B. (1985) Structure and biological activity of heparin. *Adv. Carbohydr. Chem. Biochem.* **43,** 51–134
3. Ampofo, S. A., Wang, H. M., and Linhardt, R. J. (1991) Disaccharide compositional analysis of heparin and heparan sulfate using capillary zone electrophoresis. *Anal. Biochem.* **199,** 249–255
4. Velve-Casquillas, G., Le Berre, M., Piel, M., and Tran, P. T. (2010) Microfluidic tools for cell biological research. *Nano Today* **5,** 28–47
5. Chi, L., Amster, J., and Linhardt, R. J. (2005) Mass spectrometry for the analysis of highly charged sulfated carbohydrates. *Curr. Anal. Chem.* **1,** 223–240
6. Conrad, H. E. (1998) Heparin Binding Proteins, 183–411, Academic Press, San Diego, CA
7. Vanboeckel, C. A., and Petitou, M. (1993) The unique antithrombin-III binding domain of heparin–a lead to new synthetic antithrombotics. *Angew. Chem. Int. Ed. Engl.* **32,** 1671–1690
8. Petitou, M., Mourey, L., Samama, J. P., and Pascal, M. (1993) Molecular interaction of synthetic oligosaccharides with antithrombin-III. *J. Cell. Biochem.* **17A,** 369–369
9. Hess, G. (2008) Congress investigates tainted heparin. *Chem. Eng. News* **86,** 8
10. Kemsley, J. (2008) Heparin undone. *Chem. Eng. News* **86,** 38–40
11. Liu, H., Zhang, Z., and Linhardt, R. J. (2009) Lessons learned from the contamination of heparin. *Nat. Prod. Rep.* **26,** 313–321
12. Yang, B., Solakyildirim, K., Chang, Y., and Linhardt, R. (2010) Hyphenated techniques for the analysis of heparin and heparan sulfate. *Anal. Bioanal. Chem.* **399,** 541–557
13. Wolff, J. J., Amster, I. J., Chi, L., and Linhardt, R. J. (2007) Electron detachment dissociation of glycosaminoglycan tetrasaccharides. *J. Am. Soc. Mass. Spectrom.* **18,** 234–244
14. Wolff, J. J., Chi, L., Linhardt, R. J., and Amster, I. J. (2007) Distinguishing glucuronic from iduronic acid in glycosaminoglycan tetrasaccharides by using electron detachment dissociation. *Anal. Chem.* **79,** 2015–2022
15. Leach, F. E., 3rd, Wolff, J. J., Laremore, T. N., Linhardt, R. J., and Amster, I. J. (2008) Evaluation of the experimental parameters which control electron detachment dissociation, and their effect on the fragmentation efficiency of glycosaminoglycan carbohydrates. *Int. J. Mass Spectrom.* **276,** 110–115
16. Wolff, J. J., Laremore, T. N., Aslam, H., Linhardt, R. J., and Amster, I. J. (2008) Electron-induced dissociation of glycosaminoglycan tetrasaccharides. *J. Am. Soc. Mass. Spectrom.* **19,** 1449–1458
17. Wolff, J. J., Laremore, T. N., Busch, A. M., Linhardt, R. J., and Amster, I. J. (2008) Influence of charge state and sodium cationization on the electron detachment dissociation and infrared multiphoton dissociation of glycosaminoglycan oligosaccharides. *J. Am. Soc. Mass. Spectrom.* **19,** 790–798
18. Wolff, J. J., Laremore, T. N., Busch, A. M., Linhardt, R. J., and Amster, I. J. (2008) Electron detachment dissociation of dermatan sulfate oligosaccharides. *J. Am. Soc. Mass. Spectrom.* **19,** 294–304
19. Wolff, J. J., Leach, F. E., 3rd, Laremore, T. N., Kaplan, D. A., Easterling, M. L., Linhardt, R. J., and Amster, I. J. (2010) Negative electron transfer dissociation of glycosaminoglycans. *Anal. Chem.* **82,** 3460–3466
20. Leach, F. E., Wolff, J. J., Xiao, Z., Ly, M., Laremore, T. N., Arungundram, S., Al-Mafraji, K., Venot, A., Boons, G.-J., Linhardt, R. J., and Amster, I. J. (2011) Negative electron transfer dissociation Fourier transform mass spectrometry of glycosaminoglycan carbohydrates. *Eur. J. Mass Spectrom.* **17,** 167–176
21. Leach, F. E., 3rd, Xiao, Z., Laremore, T. N., Linhardt, R. J., and Amster, I. J. (2011) Electron detachment dissociation and infrared multiphoton dissociation of heparin tetrasaccharides. *Int. J. Mass Spectrom.* **308,** 253–259
22. Oh, H. B., Leach, F. E., 3rd, Arungundram, S., Al-Mafraji, K., Venot, A., Boons, G.-J., and Amster, I. J. (2011) Multivariate analysis of electron detachment dissociation and infrared multiphoton dissociation mass spectra of heparan sulfate tetrasaccharides differing only in hexuronic

acid stereochemistry. *J. Am. Soc. Mass. Spectrom.* **22,** 582–590
23. Zaia, J., McClellan, J. E., and Costello, C. E. (2001) Tandem mass spectrometric determination of the 4S/6S sulfation sequence in chondroitin sulfate oligosaccharides. *Anal. Chem.* **73,** 6030–6039
24. McClellan, J. E., Costello, C. E., O'Connor, P. B., and Zaia, J. (2002) Influence of charge state on product ion mass spectra and the determination of 4S/6S sulfation sequence of chondroitin sulfate oligosaccharides. *Anal. Chem.* **74,** 3760–3771
25. Zaia, J., and Costello, C. E. (2003) Tandem mass spectrometry of sulfated heparin-like glycosaminoglycan oligosaccharides. *Anal. Chem.* **75,** 2445–2455
26. Zaia, J., Li, X. Q., Chan, S. Y, and Costello, C. E. (2003) Tandem mass spectrometric strategies for determination of sulfation positions and uronic acid epimerization in chondroitin sulfate oligosaccharides. *J. Am. Soc. Mass. Spectrom.* **14,** 1270–1281
27. Naggar, E. F., Costello, C. E., and Zaia, J. (2004) Competing fragmentation processes in tandem mass spectra of heparin-like glycosaminoglycans. *J. Am. Soc. Mass. Spectrom.* **15,** 1534–1544
28. Miller, M. J., Costello, C. E., Malmström, A., and Zaia, J. (2006) A tandem mass spectrometric approach to determination of chondroitin/dermatan sulfate oligosaccharide glycoforms. *Glycobiology* **16,** 502–513
29. Bielik, A. M., and Zaia, J. (2011) Multistage tandem mass spectrometry of chondroitin sulfate and dermatan sulfate. *Int. J. Mass Spectrom.* **305,** 131–137
30. Saad, O. M., and Leary, J. A. (2004) Delineating mechanisms of dissociation for isomeric heparin disaccharides using isotope labeling and ion trap tandem mass spectrometry. *J. Am. Soc. Mass. Spectrom.* **15,** 1274–1286
31. Saad, O. M., and Leary, J. A. (2005) Heparin sequencing using enzymatic digestion and ESI-MS^n with HOST: A heparin/HS oligosaccharide sequencing tool. *Anal. Chem.* **77,** 5902–5911
32. Ly, M., Leach, F. E., 3rd, Laremore, T. N., Toida, T., Amster, I. J., and Linhardt, R. J. (2011) The proteoglycan bikunin has a defined sequence. *Nat. Chem. Biol.* **7,** 827–833
33. Lohse, D. L., and Linhardt, R. J. (1992) Purification and characterization of heparin lyases from *Flavobacterium heparinum*. *J. Biol. Chem.* **267,** 24347–24355
34. Conrad, H. E. (2001) Nitrous acid degradation of glycosaminoglycans. *Curr. Protoc. Mol. Biol.* 2001 May Chapter 17, Unit 17.22A
35. Takagaki, K., Kojima, K., Majima, M., Nakamura, T., Kato, I., and Endo, M. (1992) Ion-spray mass-spectrometric analysis of glycosaminoglycan oligosaccharides. *Glycoconj. J.* **9,** 174–179
36. Jones, C. J., Beni, S., Limtiaco, J. F., Langeslay, D. J., and Larive, C. K. (2011) Heparin characterization: Challenges and solutions. *Annu. Rev. Anal. Chem.* **4,** 439–465
37. Meissen, J. K., Sweeney, M. D., Girardi, M., Lawrence, R., Esko, J. D., and Leary, J. A. (2009) Differentiation of 3-*O*-sulfated heparin disaccharide isomers: Identification of structural aspects of the heparin CCL2-binding motif. *J. Am. Soc. Mass. Spectrom.* **20,** 652–657
38. Orlando, R., Allen Bush, C., and Fenselau, C. (1990) Structural analysis of oligosaccharides by tandem mass spectrometry: Collisional activation of sodium adduct ions. *Biol. Mass Spectrom.* **19,** 747–754
39. Staempfli, A., Zhou, Z., and Leary, J. A. (1992) Gas-phase dissociation mechanisms of dilithiated disaccharides: tandem mass spectrometry and semiempirical calculations. *J. Org. Chem.* **57,** 3590–3594
40. Desaire, H., and Leary, J. A. (2001) The effects of coordination number and ligand size on the gas phase dissociation and stereochemical differentiation of cobalt-coordinated monosaccharides. *Int. J. Mass Spectrom.* **209,** 171–184
41. Gaucher, S. P., and Leary, J. A. (1999) Determining anomericity of the glycosidic bond in Zn(II)-diethylenetriamine-disaccharide complexes using MS^n in a quadrupole ion trap. *J. Am. Soc. Mass Spectrom.* **10,** 269–272
42. Harvey, D. (2001) Ionization and collision-induced fragmentation of *N*-linked and related carbohydrates using divalent cations. *J. Am. Soc. Mass Spectrom.* **12,** 926–937
43. Zhou, Z., Ogden, S., and Leary, J. A. (1990) Linkage position determination in oligosaccharides: mass spectrometry (MS/MS) study of lithium-cationized carbohydrates. *J. Org. Chem.* **55,** 5444–5446
44. Tissot, B., Gasiunas, N., Powell, A. K., Ahmed, Y., Zhi, Z.-L., Haslam, S. M., Morris, H. R., Turnbull, J. E., Gallagher, J. T., and Dell, A. (2007) Toward GAG glycomics: Analysis of highly sulfated heparins by MALDI-TOF mass spectrometry. *Glycobiology* **17,** 972–982
45. Zhang, Z., and Linhardt, R. J. (2009) Sequence analysis of native oligosaccharides using negative ESI tandem MS. *Curr. Anal. Chem.* **5,** 225–237
46. Kailemia, M. J., Li, L., Ly, M., Linhardt, R. J., and Amster, I. J. (2012) Complete mass spectral characterization of a synthetic ultralow-molecular-weight heparin using collision-induced dissociation. *Anal. Chem.* **84,** 5475–5478
47. Xiao, Z., Zhao, W., Yang, B., Zhang, Z., Guan, H., and Linhardt, R. J. (2011) Heparinase 1 selectivity for the 3,6-di-*O*-sulfo-2-deoxy-2-sulfamido-α-D-glucopyranose(1,4)2-*O*-sulfo-α-L-idopyranosyluronic acid (GlcNS3S6S-IdoA2S) linkages. *Glycobiology* **21,** 13–22
48. Liu, R., Xu, Y., Chen, M., Weïwer, M., Zhou, X., Bridges, A. S., DeAngelis, P. L., Zhang, Q., Linhardt, R. J., and Liu, J. (2010) Chemoenzymatic design of heparan sulfate oligosaccharides. *J. Biol. Chem.* **285,** 34240–34249
49. Ceroni, A., Maass, K., Geyer, H., Geyer, R., Dell, A., and Haslam, S. M. (2008) GlycoWorkbench: A tool for the computer-assisted annotation of mass spectra of glycans. *J. Proteome Res.* **7,** 1650–1659
50. Domon, B., and Costello, C. E. (1988) A systematic nomenclature for carbohydrate fragmentations in FAB-MS MS spectra of glycoconjugates. *Glycoconj. J.* **5,** 397–409
51. Hofmeister, G. E., Zhou, Z., and Leary, J. A. (1991) Linkage position determination in lithium-cationized disaccharides: tandem mass spectrometry and semiempirical calculations. *J. Am. Chem. Soc.* **113,** 5964–5970
52. Spengler, B., Dolce, J. W., and Cotter, R. J. (1990) Infrared laser desorption mass spectrometry of oligosaccharides: fragmentation mechanisms and isomer analysis. *Anal. Chem.* **62,** 1731–1737
53. Leymarie, N., and Zaia, J. (2012) Effective use of mass spectrometry for glycan and glycopeptide structural analysis. *Anal. Chem.* **84,** 3040–3048